

NATIONAL AERONAUTICS AND SPACE ADMINISTRATION

*Technical Report No. 32-867**Laminar Boundary-Layer Heat Transfer from
a Partially-Ionized Monatomic Gas by
the Similarity Approach**L. H. Back*

FACILITY FORM 602

<u>N 66-16 747</u> (ACCESSION NUMBER)	<u>1</u> (THRU)
<u>31</u> (PAGES)	<u>33</u> (CODE)
<u>CR 70035</u> (NASA CR OR TMX OR AD NUMBER)	<u>33</u> (CATEGORY)

GPO PRICE \$ _____

CFSTI PRICE(S) \$ _____

Hard copy (HC) 8.00Microfiche (MF) .20

653 July 65

JET PROPULSION LABORATORY
CALIFORNIA INSTITUTE OF TECHNOLOGY
PASADENA, CALIFORNIA

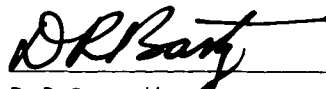
February 1, 1966

NATIONAL AERONAUTICS AND SPACE ADMINISTRATION

Technical Report No. 32-867

*Laminar Boundary-Layer Heat Transfer from
a Partially-Ionized Monatomic Gas by
the Similarity Approach*

L. H. Back

A handwritten signature in black ink, appearing to read "D. R. Bartz", is positioned above a horizontal line.

D. R. Bartz, Manager
Research and Advanced Concepts

JET PROPULSION LABORATORY
CALIFORNIA INSTITUTE OF TECHNOLOGY
PASADENA, CALIFORNIA

February 1, 1966

Copyright © 1966
Jet Propulsion Laboratory
California Institute of Technology
Prepared Under Contract No. NAS 7-100
National Aeronautics & Space Administration

CONTENTS

I. Introduction	1
II. Similarity Considerations	3
A. Wall-Boundary Conditions	5
B. Free-Stream Conditions	5
C. Net Ion Production Rate	6
D. Transport Property Dependence	6
III. Ionization Effects on Heat Transfer from a Low Speed Flow with Constant Free-stream Velocity	11
A. Solution for Diffusion Rate Large Compared to the Net Ion Production Rate	11
B. Solution for Local Equilibrium	13
C. Comparison of Predictions	14
IV. Heat Transfer Prediction with Variable Free-Stream Velocity	15
V. Conclusions	16
Appendixes	
A. Thermodynamic Properties	17
B. Derivation of Some Equations	18
C. Transport Properties	19
Nomenclature	24
References	25

TABLES

1. Values of $\frac{g'_{w}/(2)^{1/2}}{1 - g_w}$ for local equilibrium of argon at a pressure of 0.1 atm, 350°K wall temperature, and $PR = 2/3$.	15
C-1. Rigid elastic-sphere atom-atom and ion-atom collision cross-sections for monatomic gases	22

FIGURES

1. Dependence of the heat transfer parameter on Lewis number and free-stream ionization energy fraction for $Pr = 2/3$ and a highly cooled wall, $g_w = 0$, $z_{iw} = 0$	7
2. Variation of thermal conductivity with temperature for argon	8
3. Variation of viscosity with temperature for argon	9
4. Variation of density-viscosity product ratio, Prandtl and Lewis numbers with temperature for argon at a pressure of 0.1 atm and free-stream temperature of 12,000°K	10
5. Variation of the parameters ε and λ and ion mass fraction c_i with temperature for argon at a pressure of 0.1 atm	10
6. Variation of the integral F_3 (Le , Pr) and function χ (Le , Pr) with Lewis number for $Pr = 2/3$	13
7. Comparison of the limiting cases for argon at a pressure of 0.1 atm, wall temperature of 350°K and $Pr = 2/3$	14
C-1. Collision cross-sections for argon	21

ABSTRACT

N 16747
Laminar boundary-layer heat transfer from a singly-ionized monatomic gas to a highly cooled wall, with no applied external electric or magnetic fields, is analyzed by the similarity solution approach. The gas is assumed to be electrically neutral with ambipolar diffusion by ion-electron pairs. In addition, equal electron and atom-ion temperatures are assumed, and sheath effects are not considered. From existing perfect gas similarity solutions, the number of parameters that need to be investigated is reduced to those directly related to ionization effects. Solutions for the limiting cases of a large diffusion rate compared to the net production rate of ions, and for local equilibrium, are obtained for constant Prandtl number and a range of Lewis numbers. An approximate prediction method is then suggested to account for variable free-stream velocity and ionization effects in a flow over a highly cooled wall.

Author

I. INTRODUCTION

This analytical study is concerned with the effect of ionization on laminar boundary-layer heat transfer from a steady flow of a singly-ionized monatomic gas to a highly cooled wall with no applied external electric or magnetic fields. A treatment of the problem entails a knowledge of the thermodynamic state of the gas, reaction rates and transport properties in addition to accounting for the effects of variable free-stream velocity, range of flow speeds and variable properties across the boundary layer as a result of relatively large differences between the free-stream and cooled-wall temperatures.

Previous investigations which are subsequently described have been concerned primarily with stagnation

point heat transfer. To treat the more general case of flow over arbitrary surfaces the similarity approach, of various methods used in laminar boundary layer analyses, appears advantageous in determining the important parameters. Lees (Ref. 1) has pointed out the usefulness of similarity solutions applied on a local basis to predict heat transfer to cooled walls from variable-free-stream velocity flows of dissociated gases. In treating ionization effects, the analysis follows the theory of Fay and Kemp (Ref. 2). The gas consisting of atoms, ions and electrons, all assumed at the same temperature, is taken to be electrically neutral with ambipolar diffusion by ion-electron pairs. In the analysis, though not restricted to a particular monatomic gas, special con-

sideration is given to argon because of its use in many studies.

Although, as expected, the conditions for which similarity solutions are possible are rather limited, the similarity approach does indicate the various parameters on which the heat transfer to the wall is dependent: free-stream conditions as described by free-stream velocity and ion concentration gradient parameters; wall boundary conditions; net ion production rate; transport properties as they appear in the Prandtl and Lewis numbers and density-viscosity product; and kinetic to total energy and ionization to total energy fractions. The similarity approach is useful in conjunction with existing perfect gas similarity solutions in considering a simpler flow in which there are no free-stream velocity and free-stream ion concentration-gradients, and low speed flow is assumed. Prandtl and Lewis numbers are assumed constant across the boundary layer and a range of Lewis numbers is investigated. Because of the scarcity of recombination rate data over a large temperature range, extending down to a highly cooled wall value like 350°K , two limiting cases are considered: in one the diffusion rate in the boundary layer is assumed large compared to the net production rate of ions (sometimes referred to as frozen flow), and in the other the boundary layer is assumed to be in local equilibrium. The gas at the cooled wall is assumed in equilibrium. Finally, an approximate prediction method is presented which incorporates the simpler flow predictions to account for ionization effects into existing perfect gas similarity solutions which include variable free-stream velocity and highly cooled wall effects.

Specific attention is devoted to the correspondence between a partially ionized monatomic gas and a partially

dissociated diatomic gas as has been eluded to by other investigators, e.g., Reilly (Ref. 3), and Rutowski and Bershader (Ref. 4). However, as was noted in a review by Ludwig and Heil (Ref. 5) in 1960, no quantitative studies of ionization effects have been made which would allow a direct comparison to a dissociated diatomic gas. In this connection, Talbot's theory of the stagnation-point Langmuir probe (Ref. 6) should be mentioned, but only frozen flow was considered in treating a partially ionized monatomic gas. A later analysis by Park (Ref. 7) for partially-ionized argon has been made for the limiting cases of frozen and equilibrium flow over a flat plate and at an axisymmetric stagnation point. However, by choosing the binary mixture as heavy particles, i.e., atoms and ions, and electrons, a comparison to predictions from the ambipolar model is difficult. Finson and Kemp (Ref. 8) recently extended the theory of Fay and Kemp (Ref. 2) to stagnation-point heat transfer and found fair agreement with the measurements of Rutowski and Bershader (Ref. 4) and Reilly (Ref. 3).

Non-equilibrium effects such as unequal electron and atom-ion temperature and non-equilibrium conditions at the edge of the boundary layer and at the wall are not considered; in addition, radiation and a molecular description of the plasma in a sheath region next to a cooled wall where electrical effects become important, are not included. The sheath thickness, which is of the order of a Debye length, is assumed to be negligibly small compared to the boundary-layer thickness. The importance of these effects has been investigated to a small extent in a boundary layer flow. In particular, Camac and Kemp (Ref. 9) found the effects of finite recombination rates, lack of equilibration between electron and atom-ion temperatures and the sheath region on the predicted transient heat transfer to the end wall behind a reflected shock wave in a shock tube to be small.

II. SIMILARITY CONSIDERATIONS

For axisymmetric flow of a partially ionized gas with no applied external electric or magnetic fields the laminar boundary layer equations, in which both the velocity and thermal layer thicknesses are small compared to either the body radius r for an external flow or the channel radius for an internal flow, are as follows:

Continuity equation:

$$\frac{\partial}{\partial x}(\rho u r^l) + r^l \frac{\partial}{\partial y}(\rho v) = 0 \quad (1)$$

with $l = 1$ for axisymmetric flow.

Momentum equation:

$$\rho u \frac{\partial u}{\partial x} + \rho v \frac{\partial u}{\partial y} = -\frac{dp}{dx} + \frac{\partial}{\partial y} \left(\mu \frac{\partial u}{\partial y} \right) \quad (2)$$

Energy equation:

$$\rho u \frac{\partial H_t}{\partial x} + \rho v \frac{\partial H_t}{\partial y} = \frac{\partial}{\partial y} \left[-q_c - q_d + \mu \frac{\partial}{\partial y} \left(\frac{u^2}{2} \right) \right] \quad (3)$$

Conservation equation for each species:

$$\rho u \frac{\partial c_i}{\partial x} + \rho v \frac{\partial c_i}{\partial y} = \frac{\partial}{\partial y} (-\rho_i V_i) + w_i \quad (4)$$

By taking $l = 0$ in Eq. (1) the analysis is applicable to flow over a plane surface. For an electrically neutral, singly ionized, monatomic gas consisting of atoms, ions and electrons, all at the same temperature, the equilibrium thermodynamic relations and mass and energy fluxes are as follows:

Equation of state:

$$p = (1 + c_i) \rho R T \quad (5)$$

Enthalpy, including the ionization energy $c_i I$:

$$H = \sum c_i H_i = \frac{5}{2} R (1 + c_i) T + c_i I \quad (6)$$

Diffusive mass flux of ions $\rho_i V_i$ for ambipolar diffusion by ion-electron pairs (Fick's law):

$$\rho_i V_i = -\rho D_{am} \frac{\partial c_i}{\partial y} \quad (7)$$

Conductive heat flux:

$$q_c = -k \frac{\partial T}{\partial y} = -\frac{k}{\bar{c}_p} \left[\frac{\partial H_t}{\partial y} - \frac{\partial}{\partial y} \left(\frac{u^2}{2} \right) - \left(1 + \frac{5}{2} \frac{RT}{I} \right) I \frac{\partial c_i}{\partial y} \right] \quad (8)$$

where

$$\bar{c}_p = \frac{5}{2} R (1 + c_i)$$

Diffusive energy flux:

$$q_d = \sum \rho c_i V_i H_i = -\rho D_{am} \left(1 + \frac{5}{2} \frac{RT}{I} \right) I \frac{\partial c_i}{\partial y} \quad (9)$$

These relations including intermediate steps leading to some of the final forms are discussed in Appendixes A and B. Since these relations are conveniently expressed in terms of the ion mass fraction, c_i , we need only consider the ion conservation equation in conjunction with the continuity, momentum and energy equations. The ion mass fraction is also the fraction of atoms ionized which usually appears in the literature as α . By introducing the Prandtl and Lewis numbers defined by

$$Pr = \frac{\mu \bar{c}_p}{k}; \quad Le = \frac{\rho D_{am} \bar{c}_p}{k} \quad (10)$$

the energy and ion conservation equations are

$$\begin{aligned} \rho u \frac{\partial H_t}{\partial x} + \rho v \frac{\partial H_t}{\partial y} = \frac{\partial}{\partial y} \left[\frac{\mu}{Pr} \frac{\partial H_t}{\partial y} + \mu \left(1 - \frac{1}{Pr} \right) \frac{\partial}{\partial y} \left(\frac{u^2}{2} \right) \right. \\ \left. + \frac{\mu}{Pr} (Le - 1) \left(1 + \frac{5}{2} \frac{RT}{I} \right) I \frac{\partial c_i}{\partial y} \right] \quad (11) \end{aligned}$$

$$\rho u \frac{\partial c_i}{\partial x} + \rho v \frac{\partial c_i}{\partial y} = \frac{\partial}{\partial y} \left[\mu \frac{Le}{Pr} \frac{\partial c_i}{\partial y} \right] + w_i \quad (12)$$

Note that in the Prandtl and Lewis numbers k is the thermal conductivity that a chemically frozen mixture would have if no chemical reactions took place. In the literature it is often referred to as the frozen or translational value. The ratio $(Pr/Le) = (\nu/D_{am})$ is also referred to as the Schmidt number.

With the specification of the net production rate of ions per unit volume, w_i , transport properties and boundary conditions, Eq. (1, 2, 11 and 12) constitute a system of coupled equations for the velocity, enthalpy and ion mass fraction distributions. These equations are identical in form to those for a partially dissociated diatomic gas except for the following: in the energy Eq. (11) the expression

$$\left(1 + \frac{\frac{5}{2}RT}{I}\right)I$$

in the third term on the right side is replaced by

$$f(c_{p_1} - c_{p_2})dT + H_i^0$$

\bar{c}_p in Eq. (8) is replaced by

$$\bar{c}_p = c_1(c_{p_1} - c_{p_2}) + c_{p_2}$$

and the ambipolar diffusion coefficient is replaced by the binary diffusion coefficient (e.g., see Lees, Ref. 1). In these expressions the subscripts 1 and 2 refer to atoms and molecules respectively, and H_i^0 is the heat of formation of atoms.

In the similarity solution approach the velocity, total enthalpy and ion mass fraction distributions normalized to their free-stream values are assumed similar in terms of a new coordinate η normal to the surface which for low speed constant property flow over a flat plate is merely the ratio y/δ . For variable property flow over an arbitrary surface this new coordinate accounts to some extent for property variation across the boundary layer and variable free-stream conditions along the surface. By combining the Levy transformation with the Mangler transformation for axisymmetric flows as was done by

Lees the y, x coordinates are related to the new coordinates, η, ξ by

$$\eta = \frac{r^l u_e}{(2\xi)^{1/2}} \int_0^\eta \rho dy; \quad \xi = \int_0^x \rho_e \mu_e u_e r^{2l} dx \quad (13)$$

Assuming the profiles are similar in terms of η , i.e.,

$$\frac{u}{u_e} = f'(\eta), \quad \frac{H_t}{H_{t_0}} = g(\eta), \quad \frac{c_I}{c_{Ie}} = z_I(\eta)$$

and that $H_{te} = H_{t_0} = \text{constant}$, the momentum, energy and ion conservation Eq. (2, 11, 12) respectively are transformed to

$$(Cf'')' + ff'' + \beta \left[\frac{\rho_e}{\rho} - (f')^2 \right] = 0 \quad (14)$$

$$\left[\frac{C}{Pr} g' + \frac{C}{Pr} (Le - 1) \left(\frac{c_{Ie} I}{H_{t_0}} \right) (1 + \epsilon) z_I' \right]' + fg' + \frac{u_e^2}{2H_{t_0}} \left[2C \left(1 - \frac{1}{Pr} \right) f'f'' \right]' = 0 \quad (15)$$

$$\left(C \frac{Le}{Pr} z_I' \right)' + fz_I' - \Gamma f' z_I + \frac{2\xi}{u_e c_{Ie}} \frac{dw_i}{d\xi} \left(\frac{w_i}{\rho} \right) = 0 \quad (16)$$

where

$$C = \frac{\rho \mu}{\rho_e \mu_e}; \quad \beta = \frac{2\xi}{u_e} \frac{du_e}{d\xi}; \quad \Gamma = \frac{2\xi}{c_{Ie}} \frac{dc_{Ie}}{d\xi}; \quad \epsilon = \frac{\frac{5}{2}RT}{I}$$

The primes denote differentiation with respect to η . The cooled wall is assumed at a specified temperature so that with the pressure distribution specified, the enthalpy and ion mass fraction are known if the gas is assumed to be in equilibrium at the wall. For a sheath region of negligible thickness, the boundary conditions are as follows:

$$f(0) = f'(0) = 0, \quad g(0) = g_w(\xi), \quad z_I(0) = z_{Iw}(\xi) \quad \text{at } \eta = 0 \quad (17)$$

$$f'(\eta) \rightarrow 1, \quad g(\eta) \rightarrow 1, \quad z_I(\eta) \rightarrow 1 \quad \text{as } \eta \rightarrow \infty$$

The total heat flux to the wall is

$$\begin{aligned} q_{Tw} &= q_{cw} + q_{dw} = \frac{\mu_w}{Pr} \left(\frac{\partial \eta}{\partial y} \right)_w H_{t_0} \left\{ g_w' + \left[(Le - 1) \left(\frac{c_{Ie} I}{H_{t_0}} \right) (1 + \epsilon) \right] z_{Iw}' \right\} \\ &= (H_{t_0} - H_w) (\rho_e u_e) \left[\frac{r^l \mu_e}{(2\xi)^{1/2}} \right] \left(\frac{\rho_w \mu_w}{\rho_e \mu_e} \right) \left[\frac{1}{Pr} \left(\frac{g_w'}{1 - g_w} \right) + \frac{(1 - z_{Iw})}{(1 - g_w)} \frac{(Le - 1)}{Pr} \left(\frac{c_{Ie} I}{H_{t_0}} \right) (1 + \epsilon) \left(\frac{z_{Iw}'}{1 - z_{Iw}} \right) \right] \end{aligned} \quad (18)$$

Similarity solutions of Eq. (14, 15, and 16) are only possible for rather stringent requirements which involve both the wall and free-stream conditions, the net ion production rate, and transport properties. In a formal manner, these requirements are as follows:

1. $g_w = \text{constant}$
2. $z_{iw} = \text{constant}$
3. $\beta \left[\frac{\rho_e}{\rho} - (f')^2 \right]$ independent of ξ
4. $\Gamma = \left(\frac{2\xi}{c_{le}} \right) \left(\frac{dc_{le}}{d\xi} \right)$ independent of ξ
5. $\left(\frac{2\xi}{d\xi/dx} \right) \left(\frac{1}{u_e c_{le}} \right) \left(\frac{w_l}{\rho} \right)$ independent of ξ
6. $C = \frac{\rho\mu}{\rho_e\mu_e} = C(\eta)$, or a *constant*
7. Either $Pr = Pr(\eta)$, or a *constant*

$$\text{and } \left\{ \begin{array}{l} \text{either } \left\{ \begin{array}{l} \frac{u_e^2}{2H_{to}} \rightarrow 0, \text{ low speed flow limit} \\ \frac{u_e^2}{2H_{to}} \rightarrow 1, \text{ high speed flow limit} \end{array} \right. \\ \text{or } \frac{u_e^2}{2H_{to}} = \text{constant if } \beta = 0 \end{array} \right.$$

or $Pr = 1$

8. Either $Le = Le(\eta)$, or a *constant*

$$\text{and } \left\{ \begin{array}{l} \text{either } \left\{ \begin{array}{l} \frac{c_{le}I}{H_{to}} \rightarrow 0, \text{ un-ionized limit} \\ \frac{c_{le}I}{H_{to}} \rightarrow 1, \text{ fully ionized limit} \end{array} \right. \\ \text{or } \frac{c_{le}I}{H_{to}} = \text{constant if } \Gamma = 0 \end{array} \right.$$

or $Le = 1$

9. $\epsilon = \frac{5}{2} \frac{RT}{I}$ independent of ξ or $\epsilon \ll 1$

Though the majority of these requirements would not be satisfied for flow over arbitrary surfaces, it is useful to discuss them and ascertain what simplifying assumptions might be appropriate to appraise the importance of ionization effects. Though some of these requirements are interrelated, for the purpose of this discussion they can be treated separately.

A. Wall-Boundary Conditions

Since a constant wall temperature can nearly be realized in practice by wall cooling, the requirement $g_w = \text{constant}$ is satisfied. The gas is assumed to be in equilibrium at the wall, i.e., the metal wall is assumed to be a perfect catalyst. If the static pressure is constant along the surface, then from the equilibrium composition relation Eq. (A-4), the requirement $z_{iw} = \text{constant}$ is also satisfied. Alternately for a cold wall where the ion mass fraction is vanishingly small, the static pressure need not be constant to satisfy Requirement 2. As mentioned previously, wall sheath effects are not considered and electrical neutrality is assumed throughout the boundary layer.

B. Free-Stream Conditions

By using Eq. (5) and (6) the group in Requirement 3 involving the free-stream velocity gradient parameter β can be rewritten as

$$\beta \left[\frac{\rho_e}{\rho} - (f')^2 \right] = \tilde{\beta} \left\{ g - (f')^2 + [(f')^2 - z_i] \left(\frac{c_{le}I}{H_{to}} \right) \right\}$$

where

$$\tilde{\beta} = \frac{\beta (H_{to}/H_e)}{1 - (H_{to}/H_e) \left(\frac{c_{le}I}{H_{to}} \right)}$$

When the free-stream ionization energy fraction $c_{le}I/H_{to}$ is negligible, the parameter $\tilde{\beta}$ reduces to the parameter $\bar{\beta}$ of Back and Witte (Ref. 10), in which g'_w was found not to vary appreciably with $\bar{\beta}$ for accelerated flows ($\bar{\beta} > 0$) even as $\bar{\beta} \rightarrow \infty$; e.g., for a highly cooled wall, $g_w \approx 0$, the effect of infinite flow acceleration was to increase g'_w about 25% above the zero free-stream velocity gradient value. Thus, even with ionization where values of $\tilde{\beta}$

would exceed $\bar{\beta}$, the effect on heat transfer would not be appreciable.

The importance of the free-stream ion concentration gradient parameter Γ is more difficult to determine. A limiting case is that for which the free-stream ion mass fraction is assumed constant (frozen flow) so that $\Gamma = 0$ and $c_{ie}I/H_{to}$ remains constant at its initial value. This would correspond to the largest driving potential and thus, diffusive energy flux to a cooled wall from an accelerated flow ($\beta > 0$) where the free-stream ion mass fraction for isentropic flow of a gas in equilibrium diminishes in the flow direction (e.g., see Witte, Ref. 11). However, as will be seen in Section III-A, the predicted conductive heat flux, which is essentially independent of Lewis number, diminishes with $c_{ie}I/H_{to}$. The net effect of these opposing trends on the predicted total heat flux is dependent on the Lewis number. For Lewis numbers less than unity, the predicted total heat flux would be less for the larger free-stream ionization energy fraction, as can be seen in Fig. 1; conversely, for Lewis numbers greater than unity, the predicted total heat flux would be higher. Thus, for accelerated flows over cooled walls, solutions with $\Gamma = 0$ place a lower limit on the predicted total heat flux for $Le < 1$ and an upper limit for $Le > 1$. These trends would be reversed for decelerated flows ($\beta < 0$) since then the free-stream ion mass fraction for isentropic flow of a gas in equilibrium would increase in the flow direction.

C. Net Ion Production Rate

Rather than specifying the net ion production rate w_i in the boundary layer, which requires both a knowledge of the ionization and recombination processes and how the rates, in particular the recombination rate, vary over the temperature range of interest, two limiting cases can be considered. These correspond to assumptions that (1) the net ion production rate in the boundary layer is negligible compared to the diffusion rate across the boundary layer, or that (2) the rates are sufficiently large so that equilibrium exists. For the equilibrium case the ion conservation Eq. (16) is replaced by the equilibrium relation Eq. (A-4).

D. Transport Property Dependence

Requirements 6-8 depend on the variation of the transport properties k , μ , and D_{am} with temperature and also

on composition when the gas is partially ionized. A few methods are described in Appendix C from which predictions of these properties have been made. In particular, Fig. 2 and 3 show predicted values of thermal conductivity and viscosity, respectively, for argon at a pressure of 0.1 atm. Shown in Fig. 4 are predicted values of C , Pr and Le over a wall to free-stream temperature range from 350 to 12,000°K. Of these terms the one that varies the most over this temperature range is C . For temperatures up to about 8000°K, C diminishes from its wall value like $C = (T_e/T)^{1-\omega}$ since $\rho\alpha(1/T)$ and $\mu\alpha T^\omega$; for atomic argon, $\omega \cong 0.75$. For temperatures above about 8000°K the predicted rapid reduction in μ as indicated in Fig. 3 augments the decrease of C with temperature.

An estimate of the effect of C varying across the boundary layer was made by Back and Witte (Ref. 10) from the stagnation point heat transfer predictions of Bade (Ref. 12) for a high temperature unionized monatomic gas with the variation of C taken into account. Bade's heat transfer predictions were found to be nearly approximated by taking C equal to unity in the boundary layer equations and setting $\rho_w\mu_w = \rho_e\mu_e$ in the heat flux expression. This approximation was previously employed by Lees (Ref. 1). To provide better agreement between the approximate method and Bade's values, in particular for highly cooled walls $g_w \rightarrow 0$, a small correction factor $(\rho_w\mu_w/\rho_e\mu_e)^{0.1}$ can be applied; this same factor appears in the Fay and Riddell analysis (Ref. 13). These observations indicate that taking $C = 1$ in the boundary layer equations and then correcting the wall heat flux prediction by the factor $(\rho_w\mu_w/\rho_e\mu_e)^{0.1}$ for accelerated flows over highly cooled walls might be a reasonable approximation with ionization effects. Even though the variation of C across the boundary layer is larger, the predicted heat flux is rather insensitive to the magnitude of the C variation. This is indicated by the small exponent in the correction factor. For decelerated perfect gas flows the effect of variable C has not been studied for highly cooled walls so that the correction factor may not apply.

For flow over an arbitrary surface, C varies along the surface as well as across the boundary layer. Though Requirement 6 is not satisfied, the relatively weak dependence of the predicted heat flux on the variation of C would be even less, since the magnitude of the variation of C across the boundary layer would decrease in the flow direction for an accelerated flow over a cooled wall.

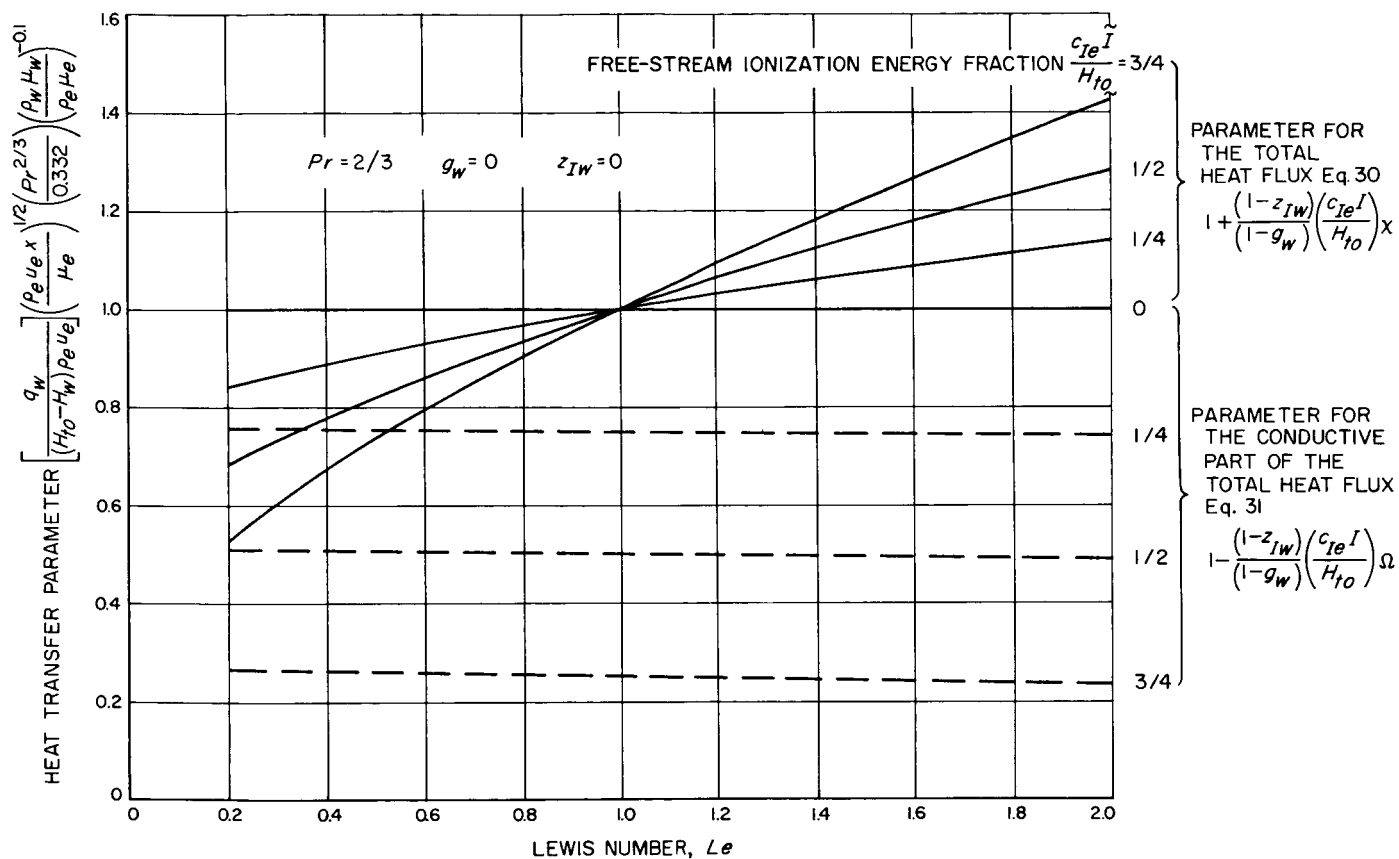


Fig. 1. Dependence of the heat transfer parameter on Lewis number and free-stream ionization energy fraction for $Pr = 2/3$ and a highly cooled wall, $g_{I0} = 0$, $z_{I0} = 0$. The predictions are for the diffusion rate assumed large compared to the net production rate of ions

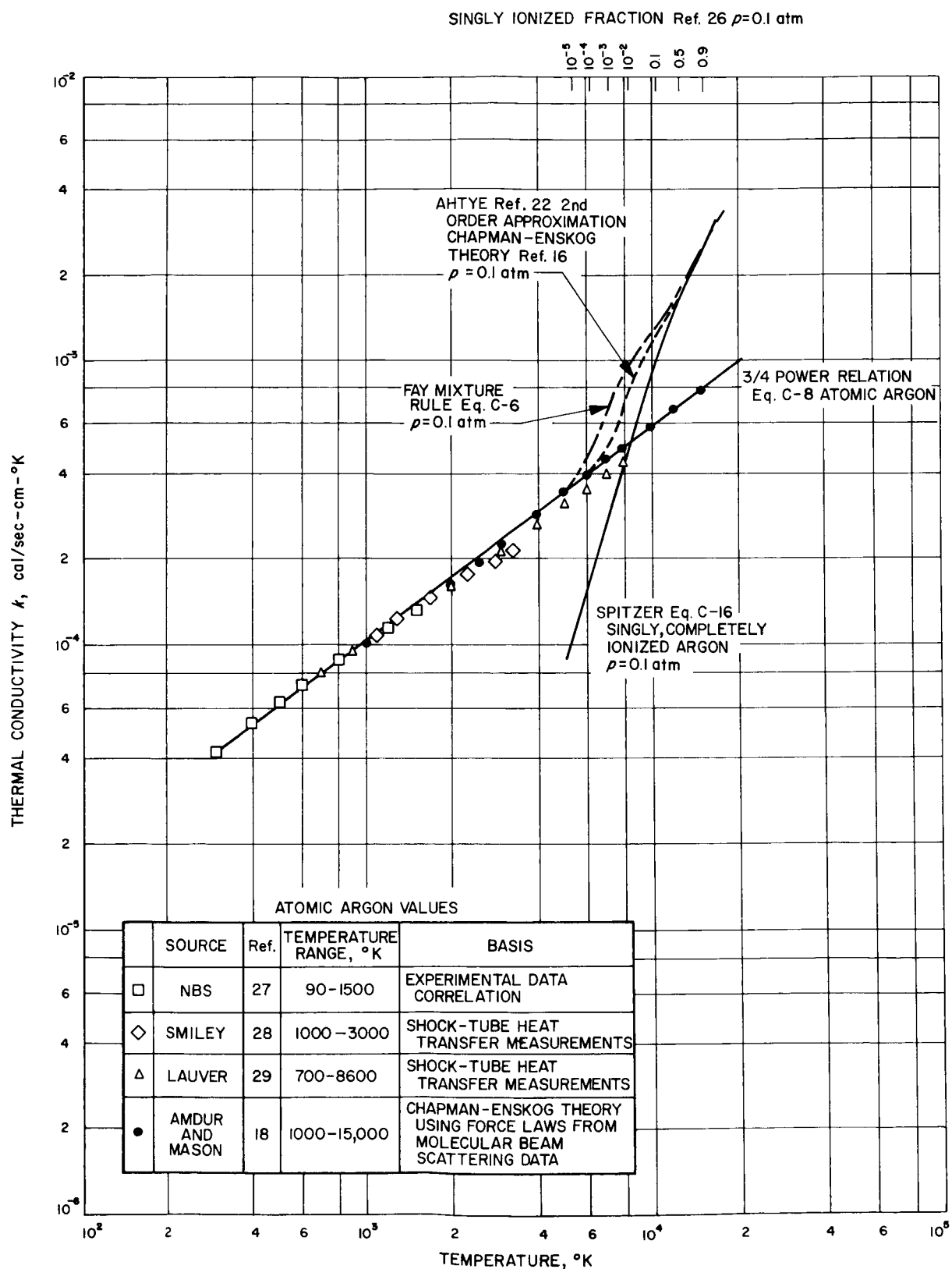


Fig. 2. Variation of thermal conductivity with temperature for argon

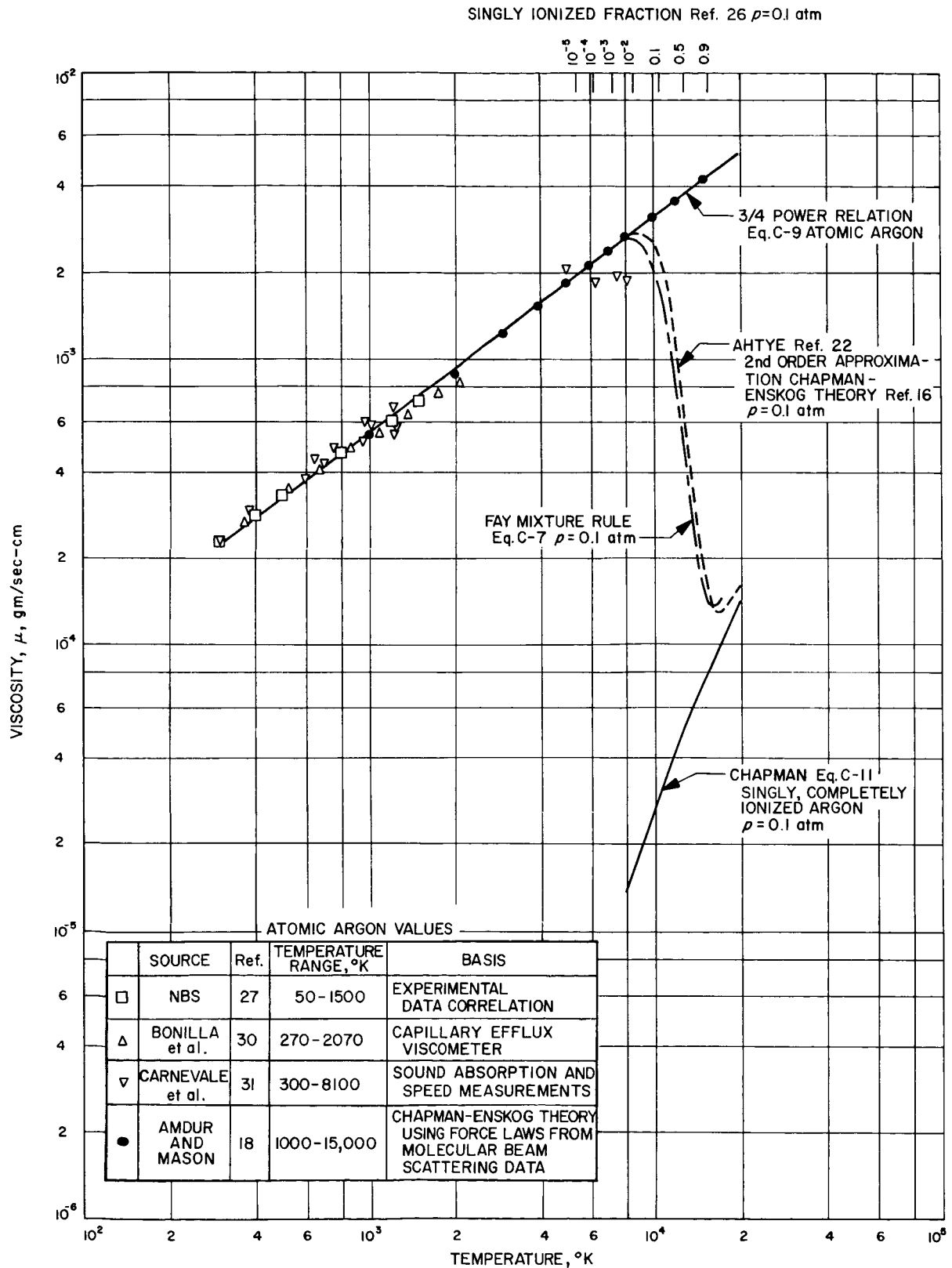


Fig. 3. Variation of viscosity with temperature for argon

In view of analytical predictions of the transport properties in the Prandtl and Lewis numbers at high temperatures where ionization effects become important, discussed in Appendix C, it seems compatible with our present knowledge to take the Prandtl and Lewis numbers constant across the boundary layer. The refinement afforded by including the actual variation of the Prandtl and Lewis numbers may be made as good transport property measurements become available. Also, as shown in Fig. 5 for argon, the parameter ϵ is small compared to unity over the temperature range of interest so that Requirement 9 is nearly satisfied.

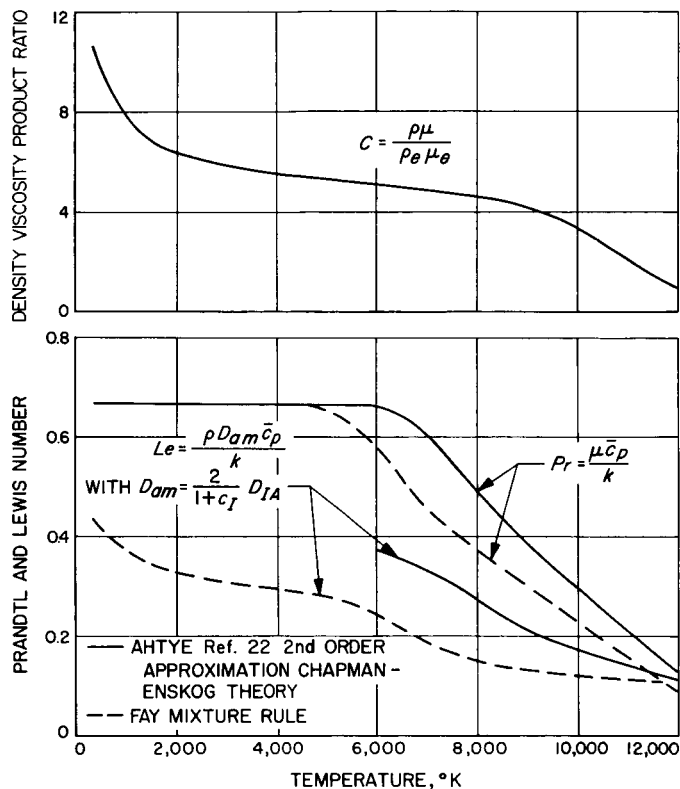


Fig. 4. Variation of density-viscosity product ratio, Prandtl and Lewis numbers with temperature for argon at a pressure of 0.1 atm and free stream temperature of 12,000°K

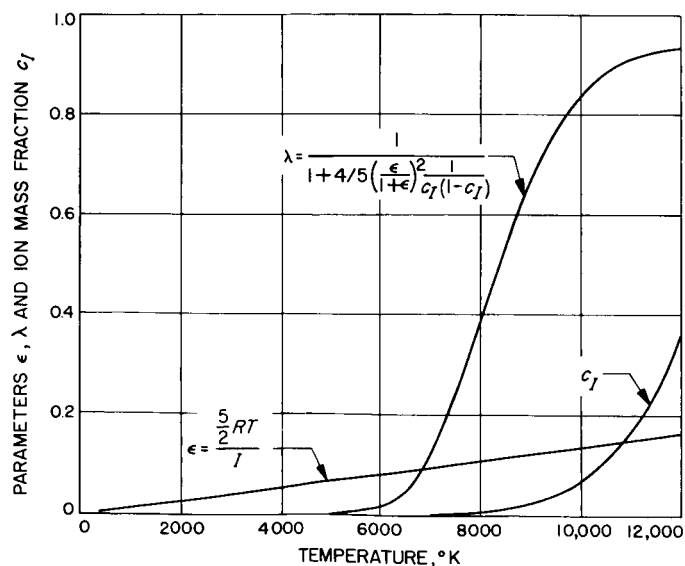


Fig. 5. Variation of the parameters ϵ and λ and ion mass fraction c_I with temperature for argon at a pressure of 0.1 atm

III. IONIZATION EFFECTS ON HEAT TRANSFER FROM A LOW SPEED FLOW WITH CONSTANT FREE-STREAM VELOCITY

To investigate the importance of ionization effects on the total heat flux the previous observations are helpful in determining appropriate simplifications. Since the effect of flow acceleration would not be appreciable as discussed in Section II-B, the free-stream velocity gradient parameter β is taken equal to zero. As a consequence it can be shown that the free-stream ion concentration gradient parameter Γ is also zero which implies that the free-stream ionization energy fraction $c_{ie}I/H_{to} = \text{constant}$. These conditions are satisfied exactly for external longitudinal flow along a cylinder and approximately for flow in the entrance region of a circular tube where the boundary layer thickness is small compared to the tube radius. The counterpart in plane flow by taking $l = 0$ is flow over a flat plate. For an isothermal wall the surface conditions are $g_w = \text{constant}$ and $z_{iw} = \text{constant}$. Further it is assumed that $C = 1$ and $Le = \text{constant}$, but not restricted to unity. A correction for C variable, discussed previously, is made later. To retain a dependence on both the Prandtl and Lewis numbers since they appear in both the energy and ion conservation Eqs. (15 and 16) the Prandtl number is taken as a constant, but not equal to unity, and low speed flow is assumed $u_e^2/2H_{to} \rightarrow 0$ so that the term in Eq. (15) involving $u_e^2/2H_{to}$ is zero. Two limiting cases are considered: (1) the diffusion rate is assumed large compared to the net ion production rate, w_i , and (2) the boundary layer is considered to be in local equilibrium. Since $\epsilon \ll 1$, ϵ is neglected compared to 1 in the first case; however, in the second case it is included for the reason discussed in Section III-B.

With the preceding assumptions the transformed Eq. (14-16) reduce to the following:

1. Diffusion rate large compared to the net production rate of ions:

$$f''' + ff'' = 0 \quad (19)$$

$$g'' + Pr(fg') = (1 - Le)\left(\frac{c_{ie}I}{H_{to}}\right)z_i'' \quad (20)$$

$$z_i'' + \frac{Pr}{Le}fz_i' = 0 \quad (21)$$

2. Local equilibrium:

$$f''' + ff'' = 0 \quad (22)$$

$$\{[1 + (Le - 1)\lambda]g'\}' + Pr(fg') = 0 \quad (23)$$

in which

$$\lambda = \left[1 + \frac{4}{5}\left(\frac{\epsilon}{1 + \epsilon}\right)^2 \frac{1}{c_i(1 - c_i)}\right]^{-1}$$

For the equilibrium case the ion conservation equation is not needed and in Appendix B, Eq. (23) is derived by expressing the ion concentration gradient in terms of the enthalpy gradient. The boundary conditions for both limiting cases are given by Eq. (17) with $g_w = \text{constant}$ and $z_{iw} = \text{constant}$.

A. Solution for Diffusion Rate Large Compared to the Net Ion Production Rate

The solution of Eqs. (20) and (21) is accomplished with f known from the Blasius solution of Eq. (19) (Ref. 14). The dimensionless enthalpy and ion mass fraction gradients at the wall are respectively

$$\frac{g_w'}{1 - g_w} = (2)^{1/2} \left[F_1 - \frac{(1 - z_{iw})}{(1 - g_w)} \frac{Pr}{Le} (Le - 1) \left(\frac{c_{ie}I}{H_{to}} \right) F_2 F_3 \right] \quad (24)$$

$$\frac{z_{iw}'}{1 - z_{iw}} = (2)^{1/2} F_2 \quad (25)$$

The functions F_1 , F_2 , and F_3 are given by

$$F_1 = \left[(2)^{1/2} \int_0^\infty \left(\frac{f''}{f_w''} \right)^{Pr} d\eta \right]^{-1} \simeq 0.332 Pr^{1/3} \quad (26)$$

$$F_2 = \left[(2)^{1/2} \int_0^\infty \left(\frac{f''}{f_w''} \right)^{Pr/Le} d\eta \right]^{-1} \simeq 0.332 \left(\frac{Pr}{Le} \right)^{1/3} \quad (27)$$

$$F_3 = \int_0^\infty f \left(\frac{f''}{f_w''} \right)^{(Pr/Le)(1 - Le)} \left[1 - \frac{\int_0^{2^{1/2}\eta} (f'')^{Pr} d\eta'}{\int_0^\infty (f'')^{Pr} d\eta'} \right] d\eta \quad (28)$$

The function F_1 can be approximated as shown from the Pohlhausen solution (Ref. 14). By evaluating the integral

in the similar function F_2 for values of Pr/Le less than 0.6, the approximation shown is accurate to within a few percent for values of Pr/Le to $\frac{1}{3}$, as it is also for values of Pr/Le to 15 (Pohlhausen solution, Ref. 14). By inserting the relations Eq. (24-27) in Eq. (18) with $C = 1$ (i.e., $\rho_w \mu_w = \rho_e \mu_e$) and then correcting for C variable by the factor $(\rho_w \mu_w / \rho_e \mu_e)^{0.1}$ discussed in Section II-D, the total heat flux to the wall is

$$q_{Tw} = (H_{to} - H_w) (\rho_e u_e) \left(\frac{r^1 \mu_e}{\xi} \right) \left(\frac{0.332}{Pr^{2/3}} \right) \left(\frac{\rho_w \mu_w}{\rho_e \mu_e} \right)^{0.1} \left[1 + \frac{(1 - z_{Iw})}{(1 - g_w)} \left(\frac{c_{Ie} I}{H_{to}} \right) \chi \right] \quad (29)$$

with

$$\chi = \frac{(Le - 1)}{Le^{1/3}} \left(1 - \frac{Pr}{Le} F_3 \right)$$

The heat transfer relation can be written in terms of familiar parameters for the flow considered in which $\xi = \rho_e \mu_e u_e r^2 x$ as

$$\left[\frac{q_{Tw}}{(H_{to} - H_w) \rho_e u_e} \right] \left(\frac{\rho_e u_e x}{\mu_e} \right)^{1/2} \left(\frac{Pr^{2/3}}{0.332} \right) \left(\frac{\rho_w \mu_w}{\rho_e \mu_e} \right)^{-0.1} = 1 + \frac{(1 - z_{Iw})}{(1 - g_w)} \left(\frac{c_{Ie} I}{H_{to}} \right) \chi \quad (30)$$

In Fig. 6, the integral F_3 and function χ are shown for $Pr = \frac{2}{3}$ over a range of Lewis numbers from 0.2 to 2.0. In evaluating F_3 and F_2 , the tabulated values from the Blasius solution, f_B and f''_B as a function of η_B (Ref. 14), could be used by replacing f , f'' and η by

$$f = \frac{f_B}{(2)^{1/2}}, \quad f'' = (2)^{1/2} f''_B \quad \text{and} \quad \eta = \frac{\eta_B}{(2)^{1/2}}$$

respectively. A 5-point Gauss-Chebyshev integration procedure was used.

The importance of ionization effects is contained in the second term on the right side of Eq. (30); for an un-ionized gas it is zero. In Fig. 1 the heat transfer parameter from Eq. (30) is shown by the solid curves for $g_w = 0$, $z_{Iw} = 0$ and $Pr = \frac{2}{3}$ over a range of Lewis numbers from 0.2 to 2.0 and free-stream ionization energy fractions from 0 to $\frac{3}{4}$. Also shown in Fig. 1 by the dashed curves is the heat transfer parameter for the conductive contribution to the total heat flux

$$\left[\frac{q_{cw}}{(H_{to} - H_w) \rho_e u_e} \right] \left(\frac{\rho_e u_e x}{\mu_e} \right)^{1/2} \left(\frac{Pr^{2/3}}{0.332} \right) \left(\frac{\rho_w \mu_w}{\rho_e \mu_e} \right)^{-0.1} = 1 - \frac{(1 - z_{Iw})}{(1 - g_w)} \left(\frac{c_{Ie} I}{H_{to}} \right) \Omega \quad (31)$$

with

$$\Omega = \frac{1}{Le^{1/3}} \left[1 + \frac{Pr}{Le} (Le - 1) F_3 \right]$$

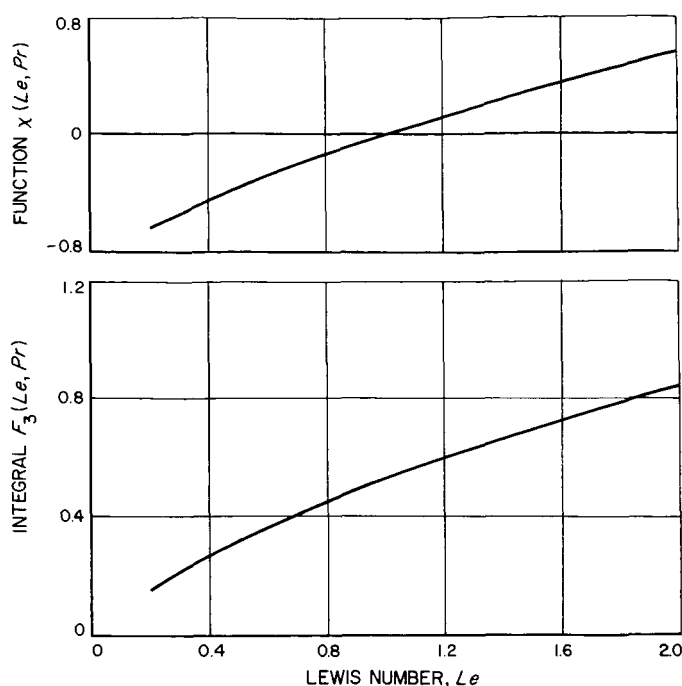


Fig. 6. Variation of the integral $F_3(Le, Pr)$ and function $\chi(Le, Pr)$ with Lewis number for $Pr = 2/3$

This contribution is essentially invariable with Lewis number, indicating a small effect of diffusion on the temperature distribution. However, this contribution is reduced as seen in Fig. 1 as the fraction of the total enthalpy in the free-stream invested in thermal enthalpy $1 - c_{te}I/H_{t0}$ decreases. The diffusive contribution, the difference between the solid and dashed curves, increases both with Lewis number and free-stream ionization energy fraction; i.e., driving potential. The sum of these contributions (solid curves) indicates the heat transfer parameter to decrease with increasing free-stream ionization energy fraction for Lewis numbers less than one. This is a result of the conductive contribution decreasing more than the diffusive contribution increases. For Lewis numbers greater than one, the reverse is true, so that the heat transfer parameter increases with the free-stream ionization energy fraction. Theoretical predictions of the Lewis number based on the ambipolar diffusion coefficient results in values less than one. These are shown in Fig. 4 and discussed in Appendix C.

Fay and Riddell (Ref. 13), in predicting stagnation point heat transfer from air including dissociation effects found the ratio

$$\frac{q_{Tw}}{(q_{Tw})_{Le=1}} = 1 + (Le^n - 1) \frac{H_D}{H_{t0}} \quad (32)$$

H_D is the dissociation enthalpy. In their calculations the Prandtl number was taken equal to 0.71 and a range of Lewis numbers from 1 to 2 was investigated. The exponent n was found to be equal to 0.63 for a frozen boundary layer with a fully catalytic wall and 0.52 for an equilibrium boundary layer. For $Pr = \frac{2}{3}$ which differs little from the value of 0.71 which was used by Fay and Riddell for air, the predicted values of χ from Eq. (29) can be approximated within a few percent by

$$\chi \simeq (Le^{0.63} - 1) \quad \text{for } 0.2 \leq Le \leq 2.0 \quad (33)$$

This close agreement is expected for Lewis numbers from 1 to 2 due to the identical form of the equations solved. However, what is rather surprising is the validity of the Fay and Riddell prediction for Lewis numbers less than unity if the dissociation enthalpy is replaced by the ionization energy $c_{te}I$, and the group $(1 - z_{iw})/(1 - g_{iw})$ included as in Eq. (30).

B. Solution for Local Equilibrium

Unlike the case where the diffusion rate was assumed large compared to the net production rate of ions, an analytic solution of Eq. (23) for the enthalpy gradient at the wall is not possible since the dependence of λ on g through the ion mass fraction makes the equation nonlinear. To indicate the variation of λ values are shown in Fig. 5 for argon at a pressure of 0.1 atm over a temperature range of 350 to 12,000°K. The values of λ were calculated by using the values of ϵ , also shown in the figure (i.e., the requirement that $\epsilon \ll 1$ was not made because of the large variation of λ with temperature), and the ion mass fraction was obtained from the equilibrium relation Eq. (A-4). Thus, it is necessary to resort to a numerical solution for a particular monatomic gas and this involves either the specification of the wall or free-stream conditions in addition to g_{iw} and z_{iw} .

A few numerical calculations have been made for argon. For a wall temperature of 350°K and a pressure of 0.1 atm, solutions were obtained for free-stream temperatures of 8000, 10,000, and 12,000°K for which the free-stream ionization energy fraction was 0.043, 0.307, and 0.614, respectively. These solutions for $Pr = \frac{2}{3}$ that span a range of Lewis numbers from 0.2 to 2.0 were obtained by solving Eq. (23) numerically with a fourth-order Runge-Kutta method on an IBM 7094 computer with f known from the Blasius solution (Ref. 14).

For local equilibrium the predicted total heat flux is due only to conduction since at the cold wall the diffusive energy flux is zero. Thus, the heat flux to the wall from

Eq. (18) with $C = 1$ (i.e., $\rho_w \mu_w = \rho_e \mu_e$) and then correcting for C variable by the factor $(\rho_w \mu_w / \rho_e \mu_e)^{0.1}$ discussed in Section II-D is

$$q_{Tw} = (H_{to} - H_w) (\rho_e u_e) \left[\frac{r^1 \mu_e}{(\xi)^{1/2}} \right] \left(\frac{\rho_w \mu_w}{\rho_e \mu_e} \right)^{0.1} \frac{1}{Pr} \left[\frac{g'_{to}/(2)^{1/2}}{1 - g_w} \right] \quad (34)$$

Values of $[g'_{to}/(2)^{1/2}]/(1 - g_w)$ are shown in Table 1.

C. Comparison of Predictions

A comparison of the limiting cases, the diffusion rate assumed large compared to the net ion production rate and local equilibrium assumed, is shown for argon in

Fig. 7 for some of the conditions at which the equilibrium solution was obtained. The difference between the predictions is small. Although the solutions in which local equilibrium was assumed were restricted to argon at a pressure of 0.1 atm and a wall temperature of 350°K, the close agreement for the few calculations made suggest that one relation, namely Eq. (30) because of its analytical form, is adequate to predict heat transfer.

Of note is that for the local equilibrium solution the corresponding equilibrium relation to Eq. (A-4) and thus, the energy equation to Eq. (23) for a partially dissociated diatomic gas are different. However, it turns out that for a partially ionized monatomic gas the difference between the limiting cases considered is small and exhibits the same trend as that found for a partially dissociated diatomic gas.

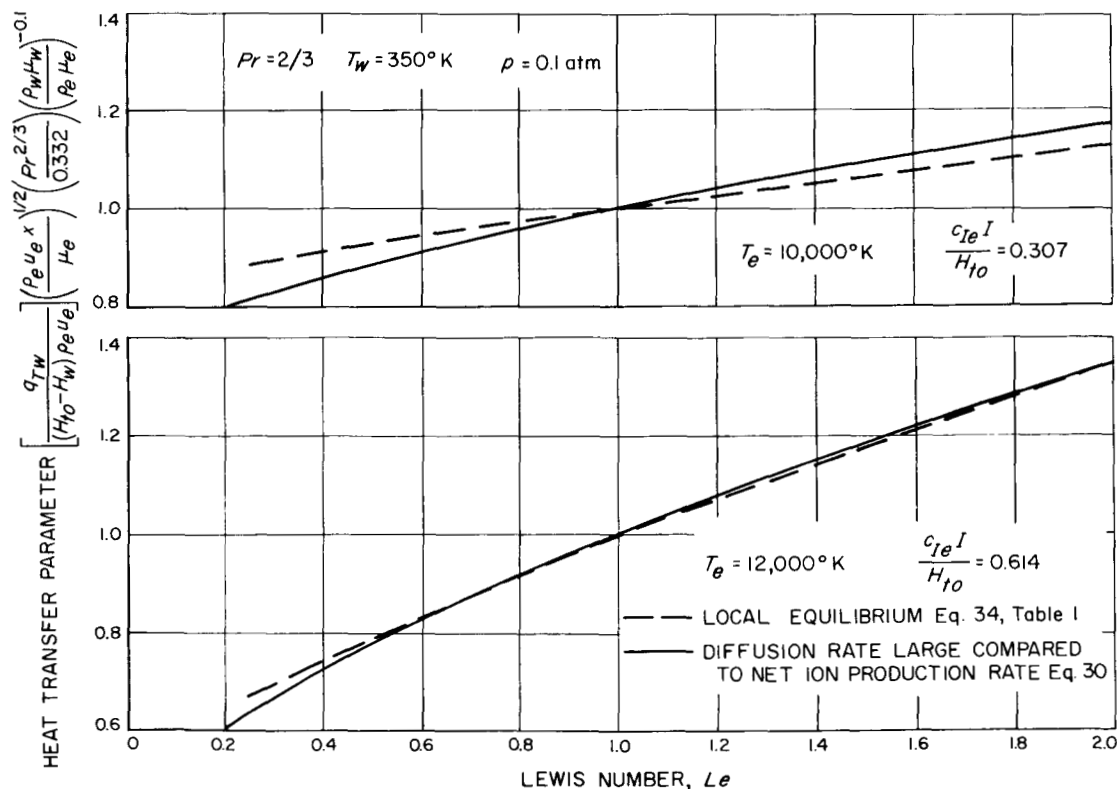


Fig. 7. Comparison of the limiting cases for argon at a pressure of 0.1 atm, wall temperature of 350°K and $Pr = 2/3$

Table 1. Values of $\frac{g'_w/(2)^{1/2}}{1 - g_w}$ for local equilibrium of argon at a pressure of 0.1 atm, 350°K wall temperature, and $Pr = 2/3$

T_e , °K	$\frac{c_{f,i}}{H_{t0}}$	g_w	$Le = 0.25$	$Le = 0.6$	$Le = 1.0$	$Le = 1.4$	$Le = 2.0$
8,000	0.043	0.0417	0.2850	0.2862	0.2876	0.2891	0.2910
10,000	0.307	0.0228	0.2552	0.2710	0.2876	0.3033	0.3255
12,000	0.614	0.00835	0.1936	0.2404	0.2876	0.3304	0.3885

IV. HEAT TRANSFER PREDICTION WITH VARIABLE FREE-STREAM VELOCITY

Having investigated the importance of ionization effects on the total heat flux in the previous section, the usefulness of that analysis in predicting heat transfer to an arbitrary surface is now considered. For an un-ionized perfect gas, Requirements 1-9 in Section II are reduced to those discussed by Back and Witte (Ref. 10), for which application of similarity solutions on a local basis to predict the conductive heat transfer to arbitrary surfaces is a reasonable approximation. This simplification is possible since the dimensionless enthalpy gradient at the wall g'_w , to which the heat flux is related, does not vary appreciably with the free-stream velocity gradient parameter β for accelerated flows over highly cooled walls. The prediction from Back and Witte (Ref. 10) for an un-ionized gas is

In this expression the length \bar{x} was introduced to cast the heat transfer parameter in a familiar form

$$\bar{x} = \frac{\xi}{\rho_e \mu_e u_e r^{2l}} = \frac{\int_0^x \rho_e \mu_e u_e r^{2l} dx}{\rho_e \mu_e u_e r^{2l}} \quad (36)$$

The group $g'_w/(1 - g_w)$ is determined from Fig. 4 of Ref. 10 for values of the free-stream velocity gradient parameter $\bar{\beta} = (T_{t0}/T_e)\beta$ and wall to total enthalpy ratio g_w . Kemp et al. (Ref. 15) have shown that the group $g'_w/(1 - g_w)$ is only slightly affected by values of $u_e^2/2H_{t0}$ ranging to $3/4$, i.e., over a substantial flow speed range, and mainly affected by β . The adiabatic wall enthalpy, H_{aw} , can be calculated from a recovery factor equal to

$$\left[\frac{q_w}{(H_{aw} - H_w) \rho_e u_e} \right] \left(\frac{\rho_e u_e \bar{x}}{\mu_e} \right)^{1/2} = \frac{1}{(2)^{1/2}} \left(\frac{g'_w}{1 - g_w} \right) \left(\frac{\rho_w \mu_w}{\rho_e \mu_e} \right)^{0.1} Pr^{-2/3} \quad (35)$$

the $\frac{1}{2}$ power of the Prandtl number (e.g., see Kemp et al., Ref. 15).

To account for ionization effects the total heat flux might then be obtained by including the term in Eq. (30) that contains the effect of ionization. The prediction is

Since the difference between the predictions for the diffusion rate assumed large compared to the net ion production rate and for assumed local equilibrium was found to be small, the use of one relation seems sufficient. Although the prediction is an approximation, it nevertheless is useful in analysis and comparison to experimental results. It also involves a minimum amount of calculation time.

$$\left[\frac{q_{rw}}{(H_{aw} - H_w) \rho_e u_e} \right] \left(\frac{\rho_e u_e \bar{x}}{\mu_e} \right)^{1/2} = \frac{1}{(2)^{1/2}} \left(\frac{g'_w}{1 - g_w} \right) \left(\frac{\rho_w \mu_w}{\rho_e \mu_e} \right)^{0.1} Pr^{-2/3} \left[1 + \frac{(1 - z_{Iw})}{(1 - g_w)} \left(\frac{c_{Ie} I}{H_{to}} \right) \chi \right] \quad (37)$$

V. CONCLUSIONS

Guided by existing laminar boundary-layer heat-transfer predictions from similarity solutions for a variable free-stream velocity, perfect-gas flow over a highly cooled wall, an estimate of the additional effect of ionization on heat transfer was made for a singly-ionized monatomic gas. Solutions for the limiting cases of the diffusion rate assumed large compared to the net ion production rate and for assumed local equilibrium indicate a predicted reduction in the heat transfer parameter below that for an un-ionized gas for Lewis numbers less than unity. The magnitude of this reduction was found to increase both with increasing free-stream ionization energy fraction and decreasing Lewis number. Predicted

Lewis numbers based on the ambipolar diffusion coefficient are less than unity.

The solutions also reveal that the Fay and Riddell stagnation-point heat transfer predictions for air including dissociation effects are equally applicable for partially-ionized monatomic gases even though their predictions were made only for Lewis numbers from 1 to 2.

Finally, an approximate prediction method which accounts for ionization effects in addition to free-stream velocity gradients and highly cooled walls is suggested.

APPENDIX A

Thermodynamic Properties

The equilibrium thermodynamic relations of an electrically neutral, singly-ionized, monatomic gas with all species at the same temperature needed in the analysis are the equation of state and expressions for the enthalpy and composition.

The equation of state for the mixture of atoms, ions and electrons each assumed to behave like a perfect gas results in Eq. (5).

From statistical mechanics the enthalpy is

$$H = \frac{5}{2} R (1 + c_I) T + c_I I + H_{elec} \quad (A-1)$$

The contribution H_{elec} is due to electronic excitational effects and depends on the ion mass fraction c_I and temperature. It is generally small; e.g., see Witte's Ref. 11 discussion on values for argon, so that essentially only ionization effects are important up to those temperatures at which the gas can be considered singly ionized. The enthalpy is then given by Eq. (6).

The equilibrium composition relation (Saha equation) is

$$\begin{aligned} \frac{c_I^2}{1 - c_I^2} &= B \left[\frac{Q_{int}(E^-) Q_{int}(A^+)}{Q_{int}(A)} \right] \frac{T^{3/2}}{p} \\ B &= \left[\frac{2 \pi m_K \kappa^{5/2}}{\hbar^2} \right]^{3/2} \\ &= 3.27 \times 10^{-7} \text{ atm } ^\circ\text{K}^{-5/2} \end{aligned} \quad (A-2)$$

T in $^\circ\text{K}$ and p in atmospheres. The Q_{int} 's are internal partition functions for the particles indicated and depend

on the statistical weights or degeneracies g_n of the particles at different energy levels E_n and temperature. A more convenient form is to write the zero-point energy of the particle (ionization energy) separately.

$$\frac{Q_{int}(E^-) Q_{int}(A^+)}{Q_{int}(A)} = \zeta e^{-I/RT} \quad (A-3)$$

Eq. (A-2) can then be written in the more familiar form

$$\frac{c_I^2}{1 - c_I^2} = B \zeta \frac{T^{3/2}}{p} e^{-I/RT} \quad (A-4)$$

In particular for argon, the only significant terms in the function ζ as noted by Witte, Ref. 11, are

$$\begin{aligned} \zeta &= \frac{g_0(E^-)}{g_0(A)} \left[g_0(A^+) + g_1(A^+) \exp\left(-\frac{E_1(A^+)}{RT}\right) \right] \\ &= 2(4 + 2e^{-2060/T}) \end{aligned} \quad (A-5)$$

Thus, Eq. (A-4) with ζ obtained from Eq. (A-5) constitutes the equilibrium relationship between ion mass fraction, pressure and temperature used in the equilibrium solution for argon. This form requires a small amount of additional calculation time than if the product $B\zeta$ is evaluated at some average value over the temperature range of interest as done in many investigations. Observation of ζ from Eq. (A-5) for argon indicates it to increase with temperature. At low temperatures, $T \rightarrow 0$, $\zeta \rightarrow 8$, and in particular at $12,000^\circ\text{K}$, $\zeta = 11.4$.

APPENDIX B

Derivation of Some Equations

The conductive heat flux relation Eq. (8) is obtained directly from the enthalpy expression Eq. (6), by differentiation.

The diffusive energy flux q_d is obtained by expanding

$$\begin{aligned} q_d &= \sum \rho c_i V_i H_i = \rho (c_I V_I H_I + c_E V_E H_E + c_A V_A H_A) \\ &= \rho c_I V_I \left(H_I + \frac{c_E}{c_I} H_E + \frac{c_A V_A}{c_I V_I} H_A \right) \end{aligned} \quad (\text{B-1})$$

The diffusion velocity V_I is taken equal to V_E since the ions and electrons are assumed to diffuse as pairs. By using the following relations, Eq. (B-1) can be written as Eq. (9). The enthalpies per unit mass of the species are

$$\begin{aligned} H_I &= \frac{5}{2} \left(\frac{\kappa}{m_I} \right) T + I; \\ H_E &= \frac{5}{2} \left(\frac{\kappa}{m_E} \right) T; \\ H_A &= \frac{5}{2} \left(\frac{\kappa}{m_A} \right) T \end{aligned} \quad (\text{B-2})$$

From the condition that the net diffusive mass flux is zero

$$\sum \rho_i V_i = \sum n_i m_i V_i = n_I m_I V_I + n_E m_E V_E + n_A m_A V_A = 0 \quad (\text{B-3})$$

By using the relations $n_I = n_E$ (electrical neutrality), $m_E < m_I$, $m_A \cong m_I$, and $V_I = V_E$, Eq. (B-3) becomes

$$\rho (c_I V_I + c_A V_A) = 0 \quad \text{or} \quad \frac{c_A V_A}{c_I V_I} = -1 \quad (\text{B-4})$$

Thus, inserting Eqs. (B-2) and (B-4) into Eq. (B-1) and noting that

$$\frac{c_E}{c_I} = \frac{n_E m_E}{n_I m_I} = \frac{m_E}{m_I}$$

the result is

$$q_d = \rho c_I V_I \left[\frac{5}{2} \left(\frac{\kappa}{m_I} \right) T + I + \left(\frac{m_E}{m_I} \right) \frac{5}{2} \left(\frac{\kappa}{m_E} \right) T - \frac{5}{2} \left(\frac{\kappa}{m_A} \right) T \right] = \rho c_I V_I \left(1 + \frac{5}{2} \frac{RT}{I} \right) I \quad (\text{B-5})$$

The gas constant $R = \kappa/m_A$. Inserting Fick's law, Eq. (7) into Eq. (B-5) gives Eq. (9).

In the local equilibrium solution in Section III, the energy Eq. (15) for $C=1$, $Pr = \text{constant}$, and $u_z^2/2H_{to} \rightarrow 0$ is

$$\left[g' + (Le - 1) \left(\frac{c_I I}{H_{to}} \right) (1 + \epsilon) z'_I \right]' + Pr (fg') = 0 \quad (\text{B-6})$$

The non-dimensionalized ion mass fraction gradient z'_I can be related to g' as follows. Since the ion mass fraction depends on temperature and pressure, Eq. (A-4) its gradient across the boundary layer where the pressure is constant is

$$\frac{\partial c_I}{\partial y} = \left(\frac{\partial c_I}{\partial T} \right)_p \frac{\partial T}{\partial y} \quad (\text{B-7})$$

By combining $\partial T/\partial y$ obtained from differentiation of the enthalpy relation Eq. (6) with Eq. (B-7) and solving for $\partial c_I/\partial y$ there results

$$\frac{\partial c_I}{\partial y} = \frac{1}{(1 + \epsilon) I} \left[\frac{1}{1 + \frac{(5/2) R (1 + c_I)}{(1 + \epsilon) I (\partial c_I / \partial T)_p}} \right] \frac{\partial H}{\partial y} \quad (\text{B-8})$$

Transforming from y to η by Eq. (13) and non-dimensionalizing c_I and H in Eq. (B-8) the energy Eq. (B-6) then becomes Eq. (15) for low speed flow ($g = H_t/H_{to} = H/H_e$) with

$$\lambda = \frac{1}{1 + \frac{(5/2) R (1 + c_I)}{(1 + \epsilon) I \left(\frac{\partial c_I}{\partial T} \right)_p}} \quad (\text{B-9})$$

To evaluate $(\partial c_i / \partial T)_p$ the equilibrium relation Eq. (A-4) is used and the result is

$$\left(\frac{\partial c_i}{\partial T} \right)_p = \frac{c_i (1 - c_i^2)}{T} \frac{I}{2RT} (1 + \varepsilon + \nu) \quad (\text{B-10})$$

The contribution of the degeneracies of the species at different energy levels is $\nu = RT/I [(T/\xi)(d\xi/dT)]$. It turns out that this contribution for argon with $d\xi/dT$ obtained from Eq. (A-5) is negligible; i.e., $\nu \ll 1$ for temperatures up to 15,000°K. Thus, λ is given by Eq. (23).

APPENDIX C

Transport Properties

To determine the variation of the Prandtl and Lewis numbers as well as $C = \rho\mu/\rho_e\mu_e$ with temperature and pressure, a knowledge of the thermal conductivity, viscosity and ambipolar diffusion coefficient is needed. Until that time when experimental measurements of these properties for monatomic gases extend into the region where ionization effects become important, use of analytical methods is required. Two such methods are considered briefly to illustrate the effects. In one method the Chapman-Enskog theory (Ref. 16) is used and the other is an approximate mixture rule proposed by Fay (Ref. 17) from a simple kinetic theory development. The latter method offers the advantage of visualizing the predicted trends and can possibly provide a method of calculating the transport properties for those monatomic bases for which rigorous predictions from the Chapman-Enskog theory have not been made. It is described briefly.

From the mixture rule of Fay the thermal conductivity and viscosity are given by

$$k = \sum_i \frac{X_i k_i}{\sum_j X_j G_{ij}} \quad (\text{C-1})$$

$$\mu = \sum_i \frac{X_i \mu_i}{\sum_j X_j G_{ij}} \quad (\text{C-2})$$

where

$$G_{ij} = \left(\frac{2m_j}{m_i + m_j} \right)^{1/2} \frac{Q_{ij}}{Q_{ii}}$$

In these expressions X_i , k_i and μ_i are the mole fraction, thermal conductivity and viscosity of the pure component i . The binary diffusion coefficient, thermal conductivity

and viscosity for the monatomic component i are related to the rigid elastic sphere cross-section Q_{ij} by

$$D_{ij} = \frac{3}{16} \frac{1}{(n_i + n_j)} \frac{1}{Q_{ij}} \left[\frac{2\pi (m_i + m_j)}{m_i m_j} \kappa T \right]^{1/2} \quad (\text{C-3})$$

$$k_i = \frac{75}{64} \frac{\kappa}{Q_{ii}} \left(\frac{\pi \kappa T}{m_i} \right)^{1/2} \quad (\text{C-4})$$

$$\mu_i = \frac{5}{16} \frac{1}{Q_{ii}} (\pi \kappa m_i T)^{1/2} \quad (\text{C-5})$$

In Ref. 2 Fay and Kemp¹ give the following form of the mixture rule which essentially weighs the contributions from the atomic gas k_a , and a singly, completely ionized gas, k_s

$$k = \frac{k_a}{1 + \left(\frac{c_I}{1 - c_I} \right) \left(\frac{Q_{IA}}{Q_{AA}} \right)} + \frac{k_s}{1 + \left(\frac{2m_E}{m_A} \right)^{1/2} \left(\frac{1 - c_I}{c_I} \right) \left(\frac{k_s}{k_a} \right) \left(\frac{Q_{EA}}{Q_{AA}} \right)} \quad (\text{C-6})$$

Because of the large mass of the ions compared to the electrons the contribution of the ions to the thermal conductivity is negligible. If the viscosity of the mixture is calculated from the mixture rule in a similar manner the result is

$$\mu = \frac{\mu_a}{1 + \left(\frac{c_I}{1 - c_I} \right) \left(\frac{Q_{IA}}{Q_{AA}} \right)} + \frac{\mu_s}{1 + \left(\frac{1 - c_I}{c_I} \right) \left(\frac{\mu_s}{\mu_a} \right) \left(\frac{Q_{IA}}{Q_{AA}} \right)} \quad (\text{C-7})$$

The contribution of the electrons to the viscosity is negligible due to their small mass. Similar to the thermal conductivity, the viscosity of the atomic and singly, completely ionized gas is denoted by μ_a and μ_s , respectively.

¹In Eq. (3.18) for Ref. 2 the ratio m_E/m_A should be corrected to $(m_E/m_A)^{1/2}$ as it appears in Avco-Everett Research Laboratory Report No. 166, March 1963.

For atomic argon experimental measurements of thermal conductivity and viscosity are shown in Fig. 2 and 3 along with power law approximations of Amdur and Mason's values (Ref. 18)

$$(k_a)_{Ar} = 5.8 \times 10^{-7} T^{3/4} \text{ cal/sec-cm-}^\circ\text{K} \quad (\text{C-8})$$

$$(\mu_a)_{Ar} = 3.1 \times 10^{-6} T^{3/4} \text{ gm/cm-sec} \quad (\text{C-9})$$

T is in $^\circ\text{K}$. From experimental end wall heat transfer measurements in a shock tube for atomic argon, before the ionization relaxation time, Camac and Feinberg (Ref. 19) found $k_a \propto T^{3/4}$ up to about 75,000 $^\circ\text{K}$.

For a singly, completely ionized gas mixture of ions and electrons Chapman (Ref. 20) has calculated the first approximation of μ_s and k_s according to the Chapman-Enskog theory for inverse square-law interaction. The electronic contribution to the viscosity is negligible compared to the ionic contribution so that μ_s is given by

$$\mu_s = \frac{5}{8} \left(\frac{1}{A_2(2)} \right) \left(\frac{m_i \kappa T}{\pi} \right)^{1/2} \left(\frac{2\kappa T}{e^2} \right)^2 \quad (\text{C-10})$$

with

$$A_2(2) = 2 \left[\ln(1 + v_{o1}^2) - \frac{v_{o1}^2}{1 + v_{o1}^2} \right]$$

For argon the viscosity is

$$(\mu_s)_{Ar} = 4.8 \times 10^{-14} \frac{T^{3/2}}{A_2(2)} \text{ gm/cm-sec} \quad (\text{C-11})$$

In the above relations and in subsequent ones, e is the electronic charge, T in $^\circ\text{K}$ and n_E in electrons per cubic centimeter are to be used with the numerical constants. The cutoff impact parameter v_{o1} is

$$v_{o1} = \frac{4}{3} \left(\frac{d}{e^2/3\kappa T} \right) = \frac{4\kappa}{e^2} \frac{T}{n_E^{1/3}} = 2.4 \times 10^3 \frac{T}{n_E^{1/3}} \quad (\text{C-12})$$

The average distance between particles is d which was taken as $1/n_E^{1/3}$. The thermal conductivity can be expressed as the sum of the ionic and electronic contributions

$$\frac{k_s}{k_E} = \left(\frac{m_E}{m_i} \right)^{1/2} \frac{1}{1 + \left(\frac{m_E}{m_i} \right)^{1/2} \frac{15}{2^{3/2}}} + \frac{1}{1 + \frac{13}{4(2)^{1/2}}} \quad (\text{C-13})$$

$$k_E = \frac{15}{4} \frac{\kappa}{(m_E m_i)^{1/2}} \mu_s \quad (\text{C-14})$$

Even though the ionic contribution is negligible compared to the electronic one, k_s is reduced below the value k_E if only electrons were present by the second term in Eq. (C-13)

$$k_s = 0.30k_E = 0.30 \left[\frac{15}{4} \frac{\kappa}{(m_E m_I)^{1/2}} \mu_s \right] \quad (\text{C-15})$$

Chapman has estimated that by including further approximations in the Chapman-Enskog theory, the overall increase in viscosity μ_s and thermal conductivity k_s should not exceed about 25% and 40%, respectively.

Another specification of the thermal conductivity is given by Spitzer (Ref. 21, pp. 87 and 88) who modified the thermal conductivity for a Lorentz gas so that the effective value for a singly, completely ionized gas is given by

$$k_s = 4.4 \times 10^{-13} \frac{T^{3/2}}{\ln \Lambda} \text{ cal/sec-cm-}^\circ\text{K} \quad (\text{C-16})$$

The Debye length l_D was used in the cutoff parameter (Ref. 21 p. 72) so that

$$\Lambda = \frac{l_D}{e^2/3\kappa T} = \frac{\left(\frac{\kappa T}{4\pi n_E e^2} \right)^{1/2}}{e^2/3\kappa T} = 1.24 \times 10^4 \frac{T^{3/2}}{n_E^{1/2}} \quad (\text{C-17})$$

For conditions such that the Debye length is smaller than the average distance between particles, Fay and Kemp (Ref. 2) suggest replacing Λ with $\frac{3}{4} v_{01}$ in Eq. (C-16) when $v_{01} \leq 16\pi$, i.e., for low temperature and high electron density.

Shown in Fig. 2 and 3 are predictions of k_s from Spitzer, Eq. (C-16) and (C-17), and μ_s from Chapman, Eq. (C-11) and (C-12), for argon at a pressure of 0.1 atm. Other calculations were made, but are not shown in the figures. Predictions from Chapman's expression for the thermal conductivity k_s were about 50% lower than Spitzer's values shown in Fig. 2. Replacing the average distance d between particles by the Debye length l_d in v_{01} , Eq. (C-12), resulted in predicted viscosity values μ_s which were about 5 to 10% below the values shown in Fig. 3. This small difference indicates the insensitivity of the prediction to the cutoff parameter chosen.

In Fig. C-1 are shown predicted collision cross-sections, ion-atom Q_{IA} , atom-atom Q_{AA} , and electron-atom Q_{EA} for argon along with a brief description of how they were obtained.

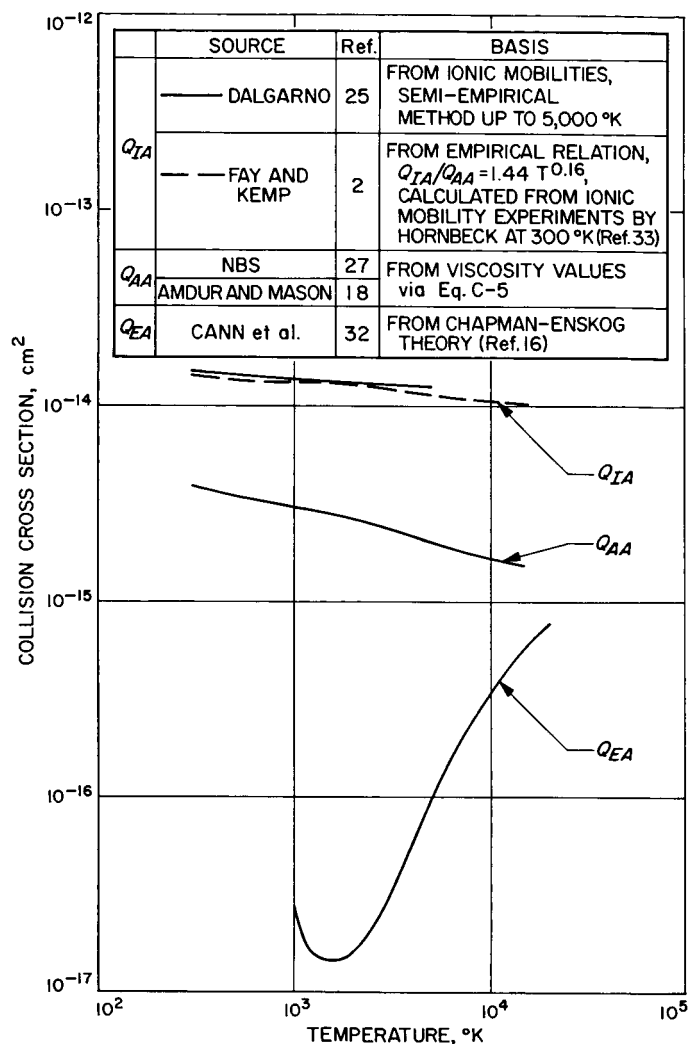


Fig. C-1. Collision cross-sections for argon

The predicted thermal conductivity from the mixture rule is seen in Fig. 2 for argon at 0.1 atm to increase above the atomic value at about 5,000°K due to the contribution of the electrons; at about 15,000°K the prediction nearly equals the completely ionized value.

As an example of a prediction from the Chapman-Enskog theory for a partially ionized gas, Ahtye's values (Ref. 22) for the second-order approximation² to k are shown in Fig. 2 for argon. Though there is close agreement with Spitzer's values at large degrees of ionization as seen in Fig. 2 at 0.1 atm in particular, Ahtye has

²The level of approximation refers to the number of terms retained in the expansion in Sonine polynomials of certain functions occurring in the distribution functions, e.g., see Ref. 16.

pointed out that the second-order values of the thermal conductivity are smaller than Spitzer's values in the singly completely ionized limit by a factor of three. This disturbing feature has apparently been reconciled by deVoto (Ref. 23) who by going to the third-order approximation in the Chapman-Enskog theory found agreement with Spitzer's values. deVoto's transport property predictions for argon cover a pressure range from 1-mm Hg to 2.5 atm. Unfortunately for comparison purposes herein, deVoto did not make predictions at 0.1 atm.

In Fig. 3 the predicted viscosity exhibits the opposite trend as the thermal conductivity; a rapid decrease below the atomic value occurs at about 8,000°K, before it again rises at about 16,000°K to coincide nearly with the completely ionized value. This decrease results from larger predicted cross-sections for ion-atom collisions than for atom-atom collisions, as seen in Fig. C-1.

The effect of higher pressures is to shift the point at which the predicted values of thermal conductivity and viscosity differ from the atomic values to higher temperatures; for lower pressures, the shift is to lower temperatures. The effect of pressure can be seen, for example, in deVoto, Ref. 23, Fig. 14.

From the predicted rise in thermal conductivity and decrease in viscosity the Prandtl number, $\mu c_p/k$, is expected to decrease with temperature; this trend is shown in Fig. 4 for argon at 0.1 atm. It is interesting to note that for a completely ionized gas the Prandtl number predicted from Chapman's values of μ_s and k_s is equal to a small value of about 0.01.

The ambipolar diffusion coefficient is usually related to the ion-atom diffusion coefficient

$$D_{am} = 2D_{IA} \quad (C-18)$$

Fay and Kemp (Ref. 2) found the following relation for a two-component mixture of atoms and ion-electron pairs by considering the momentum equation for diffusing atoms

$$D_{am} = \frac{2}{1 + c_i} D_{IA} \quad (C-19)$$

This reduces to Eq. (C-18) for small ion mass fractions. The binary diffusion coefficient for rigid elastic spheres from Eq. (C-3) then allows the calculation of the Lewis number in conjunction with k obtained from the mixture rule.

$$D_{IA} = \frac{3}{16} \left[\frac{1}{(n_A + n_i)} \right] \frac{1}{Q_{IA}} \left(\frac{4\pi kT}{m_A} \right)^{1/2} \quad (C-20)$$

The predicted Lewis number, $\rho D_{am} c_p/k$, as seen in Fig. 4 for argon at 0.1 atm, is less than unity, with an average value of about 0.25 over the temperature range shown. This relatively low value, below that for atom-atom diffusion, results from a decrease in the ion-atom diffusion coefficient due to large predicted ion-atom collision cross-sections as seen in Fig. C-1. A useful expression for the Lewis number in this regard can be obtained by combining Eqs. (C-4), (C-19 and 20) and using $c_p = 5/2R(1 + c_i)$ to give

$$Le = \frac{8}{5} \left(\frac{k_A/k}{Q_{IA}/Q_{AA}} \right) \quad (C-21)$$

In this form the Lewis number is seen to decrease both as the predicted thermal conductivity of the mixture exceeds the atomic value, and for larger predicted ion-atom than atom-atom collision cross-sections. Values of Q_{IA}/Q_{AA} shown in Table C-1 indicate that predicted Lewis numbers for other monatomic gases would be in the same range as for argon. In this connection, a private

Table C-1. Rigid elastic-sphere atom-atom and ion-atom collision cross-sections for monatomic gases

Gas	T = 300°K			T = 1000°K			T = 5000°K		
	Q_{IA}^a cm ²	Q_{AA}^b cm ²	$\frac{Q_{IA}}{Q_{AA}}$	Q_{IA}^a cm ²	Q_{AA}^c cm ²	$\frac{Q_{IA}}{Q_{AA}}$	Q_{IA}^a cm ²	Q_{AA}^c cm ²	$\frac{Q_{IA}}{Q_{AA}}$
He	73×10^{-16}	15×10^{-16}	4.9	64×10^{-16}	12×10^{-16}	5.3	55×10^{-16}	7.3×10^{-16}	7.5
Ne	$84 \times$	$21 \times$	4.0	$74 \times$	$17 \times$	4.3	$64 \times$	$13 \times$	4.9
Ar	$149 \times$	$41 \times$	3.6	$138 \times$	$31 \times$	4.5	$125 \times$	$21 \times$	6.0
Kr	$184 \times$	$53 \times$	3.5	$171 \times$	$38 \times$	4.5	$156 \times$	$28 \times$	5.6
Xe	$220 \times$	$72 \times$	3.1	$207 \times$	$50 \times$	4.1	$190 \times$	$37 \times$	5.1

^aFrom ionic mobilities, semi-empirical method of Dalgarno Ref. 25.

^bFrom viscosity values in *Handbook of Chemistry and Physics*, Chemical Rubber Publishing Co., Cleveland, Ohio, 44th Ed., pp. 2264-2267, 1963.

^cFrom viscosity values of Amdur and Mason, Ref. 18.

communication with Dr. R. Brokaw, NASA, Lewis Research Center, revealed that the predicted Lewis numbers for incipient ionization in Ref. 24 are too large by roughly a factor of two due to neglect of charge transfer effects, and instead they are in the same range as those indicated herein.

The preceeding discussion indicates a rather large predicted dependence of the transport properties on gas composition at high temperatures. Whether such large variations for monatomic gases actually occur either in magnitude or at the temperatures so indicated perhaps can be decided by experimental measurements.

NOMENCLATURE

$A_2(2)$	defined in Eq. (C-10)	V_i	diffusion velocity normal to wall of i^{th} species
c_i	mass fraction of the i^{th} species	w_i	net production rate of i^{th} species
C	dimensionless function, $\rho\mu/\rho_e\mu_e$	x	distance along wall
\bar{c}_p	mixture specific heat at constant pressure, Eq. (8)	X_i	mole fraction of i^{th} species
d	average distance between particles	y	distance normal to wall
D_{ij}	binary diffusion coefficient	z_i	dimensionless ion mass fraction, $c_{i,}/c_{i,e}$
D_{am}	ambipolar diffusion coefficient	β	free-stream velocity gradient parameter, $\frac{2\xi}{u_e} \frac{du_e}{d\xi}$
e	electronic charge	Γ	free-stream ion concentration gradient parameter, $\frac{2\xi}{c_{i,e}} \frac{dc_{i,e}}{d\xi}$
f'	dimensionless velocity, u/u_e	δ	boundary layer thickness
F	defined in Eqs. (26-28)	ε	defined in Eq. (16)
g	dimensionless total enthalpy, H_t/H_{t0} ; g'_w gradient at wall	ζ	defined in Eq. (A-5)
g_n	statistical weights or degeneracies of n^{th} energy level	η	dimensionless coordinate normal to wall, Eq. (13)
G_{ij}	defined in Eq. (C-1)	κ	Boltzmann constant
\bar{h}	Planck's constant	λ	defined in Eq. (23)
H	static enthalpy	Λ	defined in Eq. (C-17)
H_t	stagnation enthalpy, $H + u^2/2$	μ	viscosity
I	ionization energy	ν	kinematic viscosity
k	thermal conductivity	ν_{oi}	cutoff impact parameter, Eq. (C-12)
l_D	Debye length, $(\kappa T/4\pi n_E e^2)^{1/2}$	ξ	coordinate along wall, Eq. (13)
Le	Lewis number, $\rho D_{am} \bar{c}_p/k$	ρ	density
m	particle mass	v	defined in Eq. (B-10)
M	molecular weight	χ	defined in Eq. (29)
n	particle number density	ω	exponent of viscosity-temperature relation
p	static pressure	Ω	defined in Eq. (31)
Pr	Prandtl number, $\mu \bar{c}_p/k$	<i>Subscripts</i>	
q_c	conductive heat flux, $-k \partial T/\partial y$		
q_a	diffusive energy flux, $\sum \rho c_i V_i H_i$	A	atom species
q_T	total heat flux, $q_c + q_a$	aw	adiabatic wall condition
Q_{ij}	collision cross-section	e	conditions at free-stream edge of boundary layer
Q_{int}	internal partition function	E	electron species
r	body or channel radius	i	ion species
\mathcal{R}	universal gas constant	o	reservoir condition
R	gas constant, \mathcal{R}/M	s	singly, completely ionized
T	static temperature	w	wall condition
u, v	components of velocity parallel and normal to wall		

REFERENCES

1. Lees, L., "Laminar Heat Transfer Over Blunt-Nosed Bodies at Hypersonic Flight Speeds," *Jet Propulsion*, Vol. 26, pp. 259-269, April 1956.
2. Fay, J. A. and Kemp, N. H., "Theory of Heat Transfer to a Shock-Tube End-Wall from an Ionized Monatomic Gas," *Journal of Fluid Mechanics*, Vol. 21, Part 4, pp. 659-672, April 1965.
3. Reilly, J. A., "Stagnation-Point Heating in Ionized Monatomic Gases," *Physics of Fluids*, Vol. 7, No. 12, pp. 1905-1912, December 1964.
4. Rutowski, R. W., and Bershader, D., "Shock Tube Studies of Radiative Transport in an Argon Plasma," *Physics of Fluids*, Vol. 7, No. 4, pp. 568-577, April 1964.
5. Ludwig, G. and Heil, M., "Boundary-Layer Theory with Dissociation and Ionization," *Advances in Applied Mechanics*, Vol. VI, Academic Press, New York, New York, 1960.
6. Talbot, L., "Theory of the Stagnation-Point Langmuir Probe," *Physics of Fluids*, Vol. 3, No. 2, pp. 289-298, March-April, 1960.
7. Park, C., "Heat Transfer From Nonequilibrium Ionized Argon Gas," *AIAA Journal*, Vol. 2, No. 1, pp. 169-171, January 1964.
8. Finson, M. L. and Kemp, N. H., "Theory of Stagnation-Point Heat Transfer in Ionized Monatomic Gases," *Physics of Fluids*, Vol. 8, No. 1, pp. 201-204, January 1965.
9. Camac, M. and Kemp, N. H., "A Multitemperature Boundary Layer," *AIAA Paper No. 63-460*, presented at AIAA Conference of Physics of Entry into Planetary Atmospheres, August 1963.
10. Back, L. H. and Witte, A. B., "Prediction of Heat Transfer from Laminar Boundary Layers with Emphasis on Large Free-Stream Velocity Gradients and Highly Cooled Walls," *ASME Paper No. 65-HT-62*, presented at ASME-AICHE 9th National Heat-Transfer Conference, August 1965, to be published in the *ASME Journal of Heat Transfer*.
11. Witte, A. B., "Analysis of One-Dimensional Isentropic Flow with Tables for Partially Ionized Argon," *Technical Report No. 32-661*, Jet Propulsion Laboratory, Pasadena, Calif., September 30, 1964.
12. Bade, W. L., "Stagnation-Point Heat Transfer in a High-Temperature Inert Gas," *Physics of Fluids*, Vol. 5, No. 2, pp. 150-154, February 1962.
13. Fay, J. A. and Riddell, F. R., "Theory of Stagnation Point Heat Transfer in Dissociated Air," *Journal of the Aeronautical Sciences*, Vol. 25, No. 2, pp. 73-85, February 1958.
14. Schlichting, H., *Boundary Layer Theory*, McGraw-Hill Book Company, Inc., New York, New York, 4th Ed., 1960.
15. Kemp, N. H., Rose, P. H., and Detra, R. W., "Laminar Heat Transfer Around Blunt Bodies in Dissociated Air," *Journal of the Aero-Space Sciences*, Vol. 26, pp. 421-430, July 1959.
16. Hirschfelder, J. O., Curtiss, C. F., and Bird, R. B., *Molecular Theory of Gases and Liquids*, John Wiley & Sons, Inc., New York, New York, 1954.

REFERENCES (Cont'd)

17. Fay, J. A., *Hypersonic Heat Transfer in the Air Laminar Boundary Layer, in the High Temperature Aspects of Hypersonic Flow*, Ed. by W. C. Nelson, Macmillan Co., New York, New York, pp. 583-605, 1964.
18. Amdur, I., and Mason, E. A., "Properties of Gases at Very High Temperatures," *Physics of Fluids*, Vol. 1, No. 5, pp. 370-383, September-October 1958.
19. Camac, M., and Feinberg, R. M., "Thermal Conductivity of Argon at High Temperatures," *Journal of Fluid Mechanics*, Vol. 21, Part 4, pp. 673-688, April 1965.
20. Chapman, S., "The Viscosity and Thermal Conductivity of a Completely Ionized Gas," *Astrophysical Journal*, Vol. 120, No. 1, pp. 151-154, 1954.
21. Spitzer, L. Jr., *Physics of Fully Ionized Gases*, Interscience Publishers, Inc., New York, New York, 1956.
22. Ahtye, W. F., "A Critical Evaluation of Methods for Calculating Transport Coefficients of Partially and Fully Ionized Gases," NASA TN D-2611, January 1965.
23. deVoto, R. S., *Argon Plasma Transport Properties*, SUDAER No. 217, Department of Aeronautics and Astronautics, Stanford University, February 1965.
24. Brokaw, R. S., *The Lewis Number, Progress in International Research on Thermodynamic and Transport Properties*, ASME, Academic Press, Inc., New York, New York, pp. 271-278, 1962.
25. Dalgarno, A., "The Mobilities of Ions in their Parent Gases," *Philosophical Transactions of the Royal Society of London*, Vol. 250, pp. 426-439, 1957-58.
26. Drellishak, K. S., Knopp, C. F., and Cambel, A. B., *Partition Functions and Thermodynamic Properties of Argon Plasma*, AEDC-TDR-63-146, Gas Dynamics Laboratory, Northwestern University, Evanston, Illinois, August 1963.
27. *Tables of Thermal Properties of Gases*, Circular 564, National Bureau of Standards, 1955.
28. Smiley, E. F., *The Measurement of the Thermal Conductivity of Gases at High Temperature with a Shock Tube; Experimental Results in Argon at Temperatures Between 1000° and 3000°K*, Ph.D. Thesis, The Catholic University of America, 1957.
29. Lauver, M. R., *Evaluation of Shock-Tube Heat-Transfer Experiments to Measure Thermal Conductivity of Argon from 700° to 8600°K*, NASA TN D-2117, February 1964.
30. Bonilla, C. F., Wang, S. J., and Weiner, H., "The Viscosity of Steam, Heavy-Water Vapor, and Argon at Atmospheric Pressure up to High Temperatures," *ASME Transactions*, Vol. 78, pp. 1285-1289, 1956.
31. Carnevale, E. H., Larson, G. S., and Lynnworth, L. C., *Experimental Determination of Transport Properties of High Temperature Gases*, 7th Quarterly Progress Report Contract NASw-549, Parametrics, Inc., Waltham, Massachusetts, September 8, 1964.
32. Cann, G. L., Ziemer, R. W., and Marlotte, G. L., *The Hall Current Plasma Accelerator*, AIAA Paper No. 63011, presented at AIAA, Electric Propulsion Conference, Colorado Springs, Colo., March 1963.
33. Hornbeck, J. A., "The Drift Velocities of Molecular and Atomic Ions in Helium, Neon, and Argon," *Physical Review*, Vol. 84, No. 4, pp. 615-620, 1951.